

Shell-Model Combinatorial Calculations of Nuclear Level Densities* †

MANNY HILLMAN AND J. ROBB GROVER

Brookhaven National Laboratory, Upton, New York 11973

(Received 11 April 1969)

Spin-dependent nuclear level densities were calculated for selected nuclides. In each case the numbers and spins of the levels were determined from a computer-generated list of all contributing shell-model configurations. To calculate the energies of the configurations, we assumed the model nucleus to be an infinitely deep spherical well containing fermions that are noninteracting except for pairing forces, for which the BCS theory was used. Comparisons of the calculated results with experimental level densities for odd, even, and odd-mass nuclides show reasonable agreement for nuclides with $A > 50$. The results of calculative investigations of the effects of shell closings, pairing, etc., and the persistence of these effects to high excitation energies and angular momenta are reported and discussed. Comparisons of these results with those obtained from the most commonly used algebraic formula show significant disagreements in the curvature of the logarithmic energy dependence and in the spin distributions.

I. INTRODUCTION

MEASUREMENTS of the densities of nuclear levels provide information about the structure of highly excited nuclei and are also necessary for understanding and analyzing complex nuclear reactions. Both for reconciliation of known level densities with nuclear models and for reduction of the data of nuclear reactions to information about level densities, methods of calculation are needed that are useful for a wide range of masses, energies, and angular momenta. In the past, the methods tried have involved algebraic expressions representing the consequences of simple nuclear models. The most frequently used of these belong to a family of formulas the prototype of which, due to Bethe,¹ is based on a model of noninteracting fermions in the nuclear potential well. Various modifications have been made to take account of residual interactions and of the effects of grouping single-particle levels into the major shells. One such formula^{2,3} is given in Sec. III [Eq. (10)].

Drastic approximations of a purely mathematical nature have had to be made to obtain the formulas, and often their shortcomings for matching known data are overcome by parameter adjustments. The directness of the confrontation of nuclear models with level-density data suffers in consequence. Also, that the existing prescriptions can be made to fit the data for a wide range of mass numbers can not be taken as support for their accuracy outside the narrow regions of excitation energy (0–10 MeV) and angular momentum (0–5 \hbar) to which most of the experimental

knowledge of level densities is confined.^{2,4,5} Improved methods are required for exploring the structures of highly excited nuclei through their level densities.

To effect the necessary improvements, i.e., to avoid as much as possible purely mathematical approximations, we calculate the level densities numerically using a large digital computer. That such calculations could prove feasible was shown by Grover,⁶ whose calculations were confined to limited regions of the energy-angular momentum plane. Similar calculations in highly restricted systems have been carried out by several workers.^{7–9} Rabinovitch and his co-workers have performed calculations analogous to ours for molecules.¹⁰

In the next section, we review what is sought in a level-density calculation, in the light of which the model usually used has been chosen. In Sec. III is given a brief description of an algebraic approximation to the chosen model and a summary of the mathematical simplifications employed in obtaining it. Our method of numerical evaluation is described in Sec. IV, and Secs. V and VI contain comparisons of the numerical calculations with experimental data and with calculations using an algebraic expression.

II. MODEL

For the evaporation formulas presently employed, one merely needs correct average densities with respect to energy and angular momentum, and the correct average trend of the yrast levels. These requirements are modest enough to have encouraged the expecta-

* This work was performed under the auspices of the U.S. Atomic Energy Commission.

† This work was reported in part at the 155th National Meeting of the American Chemical Society, April, 1968, Abstract No. O-176.

¹ H. A. Bethe, *Rev. Mod. Phys.* **9**, 69 (1937).

² A. Gilbert and A. G. W. Cameron, *Can. J. Phys.* **43**, 1446 (1965).

³ T. Ericson, *Advan. Phys.* **9**, 425 (1960).

⁴ U. Facchini and E. Satta-Menichella, *Energia Nucl.* **15**, 54 (1968).

⁵ J. L. Cook, H. Ferguson, and A. R. de L. Musgrove, *Australian J. Phys.* **20**, 477 (1967).

⁶ J. R. Grover, *Phys. Rev.* **157**, 832 (1967).

⁷ G. Kluge, *Nucl. Phys.* **51**, 41 (1967).

⁸ L. Motz and E. Feinberg, *Phys. Rev.* **54**, 1055 (1938).

⁹ C. L. Critchfield and S. Oleksa, *Phys. Rev.* **82**, 243 (1951).

¹⁰ For example, G. Z. Whitten and B. S. Rabinovitch, *J. Chem. Phys.* **38**, 2466 (1963).

tion that a simple calculable model should be able to reconcile much of the data presently available. However, there are already data on hand that seem to require a more detailed treatment—for example, the apparent preferential evaporation of the same type of particle as the incident particle,¹¹⁻¹³ where it may be important to take account of the structure of the states involved. Therefore, the model selected should be easily extended to include those more detailed features of structure that it can be foreseen may be needed soon.

The nuclear shell model appears very promising. Each nucleon moves independently in the average potential contributed by the other $A-1$ nucleons. The depth, shape, and dimensions of the potential well are fixed by appeal to experiments: ground state spin, the energies and spins of the first few excited states, etc.

With such a model, a large set of single-particle eigenfunctions up to some reasonably high energy can easily be calculated. By permutation of the A nucleons among these eigenfunctions, with due obeisance to the required antisymmetrization, one generates a very large set of wave functions representing the ground and many excited states of the model. The energy E_β of a particular configuration β will be, since we deal with noninteracting particles, simply the sum of the eigenvalues ϵ_i of the occupied orbitals

$$E_\beta = \sum_i \epsilon_i \quad (1)$$

and the excitation energy ϵ_β is found by subtraction of the ground-state energy E_0 :

$$\epsilon_\beta = E_\beta - E_0. \quad (2)$$

One needs only to calculate the lowest-lying ten million or so ϵ_β values, sort them out by energy, take account of the magnetic degeneracies associated with angular momentum, and express the result as a zeroth-order level-density function.

In general there are nucleon-nucleon interactions that are not included in the average field. They nevertheless affect the average level densities and therefore must be taken into account. Perhaps the most important of these, and the only one included in our model, is the pairing force. Some effects are also to be expected from the quadrupole-quadrupole forces, and the average field itself might be expected to change as a function of excitation energy and angular momentum. Hopefully it will prove feasible to include these and other complications in future work.

To correct for pairing forces, we use a simple version of standard pairing theory¹⁴ that has already proved useful for describing even-odd effects in the ground and first few excited states of nuclei. By pairing force (in this paper) is meant a strong interaction between two like nucleons in orbitals that are the time reverse of each other. In the special case of a spherical nucleus, this would be an attraction between a nucleon in the orbital with angular momentum j_i and projection m_i and an identical nucleon in j_i with projection $-m_i$. The two nucleons couple to a resultant angular momentum of zero, at the same time making an additional contribution to the nuclear binding. The energy of the configuration β corrected for pairing is the following:

$$E_\beta = \sum^0 \epsilon_i + \sum' 2\tilde{\epsilon}_{i\beta}\tilde{V}_{i\beta}^2 - \tilde{\Delta}_\beta^2/G. \quad (3)$$

Here G defines the pairing force parameter, the value of which is found by appeal to experiment,

$$\tilde{\epsilon} = \epsilon - G\tilde{V}^2, \quad (4)$$

and $\tilde{V}_{i\beta}^2$ is calculated from

$$\tilde{V}_{i\beta}^2 = \frac{1}{2} \left(1 - \frac{\tilde{\epsilon}_i - \tilde{\lambda}_\beta}{[(\tilde{\epsilon}_{i\beta} - \tilde{\lambda}_\beta)^2 + \tilde{\Delta}_\beta^2]^{1/2}} \right), \quad (5)$$

$\tilde{\Delta}_\beta$ and $\tilde{\lambda}_\beta$ being obtained by solution of the pair of equations

$$\sum' 2\tilde{V}_{i\beta}^2 = \eta_\beta, \quad (6)$$

$$\sum' \{1/[(\tilde{\epsilon}_{i\beta} - \tilde{\lambda}_\beta)^2 + \tilde{\Delta}_\beta^2]^{1/2}\} = 2/G, \quad (7)$$

where η_β is the number of paired nucleons included in the range of summation. The superscript zero indicates summation over orbitals containing unpaired nucleons, and the prime summation is only over orbital pairs in which there is not an unpaired nucleon.

To illustrate the qualitative effect of the above pairing correction on the level density, we compare the zeroth order and corrected level densities on a total energy scale, as in Fig. 1(a), for an even-even nucleus. The 2Δ is approximately the energy necessary to break the first nucleon pair. At higher energies, where many pairs are broken and the effects of pairing diminish, the energy depression disappears and the two curves approach one another. Two effects operate here; (1) the number of pairs *per se* decreases and (2) the unpaired nucleons block states making them unavailable for "scattered" pairs. Shifting the sketches to make the ground states coincide then shows the over-all effect, Fig. 1(b). The corrected level-density function starts out shifted by roughly 2Δ , then rises somewhat less steeply than the uncorrected function until the effective energy shift approaches the entire energy that was contributed by pairing in the ground-state nucleus. The argument for odd mass and odd-odd nuclei goes along similar lines.

¹¹ B. L. Cohen, Phys. Rev. **92**, 1245 (1953); B. L. Cohen and E. Newman, *ibid.* **99**, 718 (1955).

¹² D. Bodansky, Ann. Rev. Nucl. Sci. **12**, 79 (1962).

¹³ N. Dudev, M. Fluss, B. Foreman, L. Kowalski, and J. M. Miller, in *Proceedings of the International Conference on Nuclear Physics, Gatlinburg, Tennessee, 1966*, edited by R. L. Becker (Academic Press Inc., New York, 1967), p. 803; C. M. Stearns, Ph.D. thesis, Columbia University, 1961 (unpublished).

¹⁴ A. M. Lane, *Nuclear Theory* (W. A. Benjamin, Inc., New York, 1964).

III. ALGEBRAIC APPROXIMATION

For many years, approximate algebraic formulas for the model have been used, so that in comparisons of level-density theory with experiment it is not clear whether it is the mathematical method or the model that is being tested. We describe, briefly, what the approximations are. Comparison with the numerical solution of the model will then help to show what the shortcomings of past analyses must have been.

The single-particle eigenvalues near the Fermi level are assumed to be equally spaced, with a density of g levels per MeV. A relatively simple approximate solution of the all-configurations problem^{15,16} described above then becomes possible. The energy dependence is found to be essentially the exponential of the square root of the excitation energy:

$$\omega(E) = \text{const} E^{-5/4} \exp[2(aE)^{1/2}]. \quad (8)$$

The constant a carries the nuclear-well information g through a constant multiplying factor:

$$g = (6/\pi^2)a. \quad (9)$$

A simple rule is picked for the distribution of the

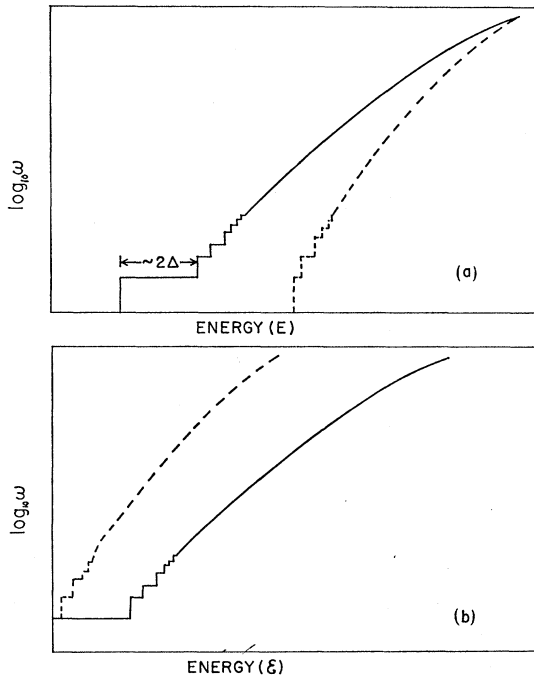


FIG. 1. The effect of pairing on the level densities of an even-even nucleus; dotted line, without pairing, solid line, with pairing; (a) with high-energy parts coinciding, showing the effect of pairing on the energies of the levels; (b) with ground states coinciding, showing the effect of pairing on the shape of the level-density curve. (More realistically, the small level-density parts of the curves should be represented as peaks instead of steps, but we employ the latter for simplicity of the figure.)

¹⁵ L. Euler, see Ref. 3.

¹⁶ G. S. Hardy and S. Ramanujan, Proc. London Math. Soc. 17, 75 (1918).

single-particle wave-function j values—for example, that their magnitudes are all the same at some average value, or that the distribution of the magnitudes obeys the simple Fermi-gas prediction. The vectors are assumed to be large in number, to be pointing in random directions, and to be coupled accordingly. Using these assumptions, the central-limit theorem can be invoked to obtain the distribution of projections* of angular momentum on a space-fixed axis. The resulting distribution of levels with respect to angular momentum is then gaussian in J with dispersion σ ,

$$\omega(E, J) = \text{const} \times (E)^{-2} \exp[2\sqrt{aE}](2J+1) \times \exp[-(J+1/2)^2/(2\sigma^2)], \quad (10)$$

except for a multiplying factor of $2J+1$. The σ connects to the nuclear-well information through the mean-square projection of the angular momentum of a single unpaired nucleon on some axis, $\langle m^2 \rangle$, times the average number of unpaired nucleons ν :

$$\sigma^2 = \nu \langle m^2 \rangle. \quad (11)$$

Equation (10) is the famous Bethe formula, first published in 1936.^{1,17}

For a long time now, Eq. (10) has been used with some simple changes to allow for pairing and shell effects. The pairing corrections have been introduced through a subtractive constant δ on the excitation energy to allow for the energy of breaking the first nucleon pair. The effect of removing the rest of the pairing energy was therefore absorbed implicitly into the value of a when the formula was fitted to experiments. Lang¹⁸ and Decowski *et al.*¹⁹ have applied the BCS pairing theory to the problem, which removes this objection, but at the expense of new expressions that are not as easy to use as the Bethe equation. Shells have been taken into account by *ad hoc* adjustment of a , either empirically² or semi-empirically²⁰ with reference to an assumed shell model. Other methods of correction have also been suggested.^{21–23}

The dispersion σ^2 has been studied experimentally beginning with the pioneering work of Huizenga and Vandenbosch.²⁴ Hard knowledge of σ^2 is still only in

¹⁷ H. A. Bethe, Phys. Rev. 50, 332 (1936).

¹⁸ D. W. Lang, Nucl. Phys. 42, 353 (1963).

¹⁹ P. Decowski, W. Grochulski, A. Marcinkowski, K. Siwek, and Z. Wilbelmi, Nucl. Phys. A110, 129 (1968).

²⁰ T. D. Newton, Can. J. Phys. 34, 804 (1956).

²¹ I. Dostrovsky, Z. Fraenkel, and G. Friedlander, Phys. Rev. 116, 683 (1959).

²² P. B. Kahn and N. Rosenzweig, Phys. Letters 22, 308 (1966).

²³ N. Rosenzweig, L. M. Bollinger, L. L. Lee, and J. P. Schiffer, in *Proceedings of the Second United Nations International Conference on Peaceful Uses of Atomic Energy* (United Nations, Geneva, 1958).

²⁴ J. R. Huizenga and R. Vandenbosch, Phys. Rev. 120, 1305 (1960); R. Vandenbosch and J. R. Huizenga, *ibid.* 120, 1313 (1960); see also subsequent work of J. Benevise, G. Merkel, and A. Mitchell, *ibid.* 141, 980 (1966); 174, 1357 (1968).

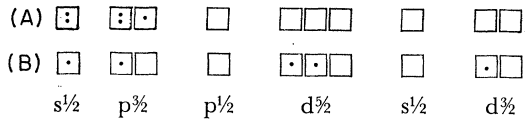


FIG. 2. Sample odometer.

a crude state, however, and most analyses use the simple Fermi-gas value.

Yrast levels do not appear in Eq. (10), which predicts levels out to $J = \infty$ at any energy. This means, of course, that to be useful the equation must carry with it a statement of its range of validity. This has sometimes been ignored in analyses of data, with misleading results.^{6,25}

IV. NUMERICAL CALCULATIONS

A. Operation of Computer Program

The computing method used for finding all of the levels and their corresponding energies is similar to the one previously used for finding the yrast levels.⁶ "Odometers" were used to scan the nuclear configurations systematically and the energy and spin distribution of each configuration was calculated, giving the number of levels of each spin for each energy.

A simple example is given in Fig. 2.

The ground-state configuration of the protons of a nucleus with $Z=5$ is given in (A). The energy of the ground-state configuration is $98.7 A^{-1/3}$ MeV, and a single level of $J = \frac{3}{2}$ occurs at this energy. An example of an excited configuration is given in (B); the corresponding energy is $219.3 A^{-1/3}$ MeV, and there are 66 levels at this energy with the spin distribution of $7(\frac{1}{2})$, $12(\frac{3}{2})$, $14(\frac{5}{2})$, $13(\frac{7}{2})$, $10(\frac{9}{2})$, $6(\frac{11}{2})$, $3(\frac{13}{2})$, and $1(\frac{15}{2})$. The excitation energy of the excited configuration is the difference between its energy and that of the ground state.

The number of times a particular spin occurs was summed for all configurations within an energy interval. Sets of spin distributions and corresponding energies were calculated separately for protons and neutrons and were then coupled. In coupling, the energies were simply added, for no neutron-proton interaction has been taken into account, and a final set of energies and spin distributions was obtained. To minimize the edge effects of binning, 500 energy bins were used for each nucleon type but ≤ 50 for the entire nucleus.

1. Calculation of Spin Distribution

Restriction to a spherically symmetric well greatly simplifies and shortens the calculations, for the orbital angular momentum \mathbf{j} becomes a good quantum number, allowing us to define a subshell.

The number of levels of given total angular mo-

mentum J for a particular configuration of subshells was calculated by finding the number of ways the component \mathbf{j} 's can couple to J . For example, all possible vectorial additions of an unpaired nucleon in a j_1 subshell coupled to an unpaired nucleon in a j_2 subshell gives one level each of spins $|j_1 - j_2|$, $|j_1 - j_2| + 1, \dots, j_1 + j_2 - 1, j_1 + j_2$. A third unpaired nucleon couples in the same way to each of the spins already developed by the first two particles, and so on. The restrictions imposed by the Pauli exclusion principle, when we must take account of two or more identical particles in the same subshell, complicate the simplicity of the above picture. We used the method described by Condon and Shortley²⁶ to solve this problem, and the result is compiled into a table given in Appendix A.

2. Calculation of Configuration Energies

The energies of the respective configurations were obtained by the BCS method²⁷ as described by Seeger²⁸ and Wahlborn.²⁹ The requisite formulas are given in Eqs. (3) to (7). The simple "blocking" method developed for one unpaired nucleon is easily extended, as also shown in Eq. (3), to cases with more than one unpaired nucleon, where all orbital pairs containing unpaired nucleons are omitted from the BCS calculation, and the corresponding single-particle energies are added to the BCS energy. When Eqs. (3), (5), and (7) are combined,²⁹ we obtain

$$E = \sum_{\text{all } i} (\bar{\epsilon}_i - \bar{\lambda}) + \bar{\lambda}N \quad (\text{or } Z) \\ - \sum' [(\bar{\epsilon}_i - \bar{\lambda})^2 + \bar{\Delta}^2]^{1/2} + \bar{\Delta}^2/G, \quad (12a)$$

where N (or Z) is the number of neutrons (or protons) in the nucleus, and the subscript β has been suppressed. The solution of Eqs. (6) and (7) for Δ and $\bar{\lambda}$ is slow because of the necessary iterations involving Eq. (4) to obtain $\bar{\epsilon}$. These extra iterations were eliminated by means of some minor approximations giving

$$E = \sum_{\text{all } i} (\epsilon_i - \lambda) + \lambda N \quad (\text{or } Z) - \sum' [(\epsilon_i - \lambda)^2 + \Delta^2]^{1/2} \\ + \Delta^2/G - 2G \sum' V_i^4, \quad (12b)$$

where Δ , λ , and V arise from Eqs. (5) to (7) with tildes deleted. Equations (12a) and (12b) were checked numerically and the resulting difference was found to be negligible.

Since configurations with much blocking usually have high energies, it is generally assumed that, above some transition energy, the superconductivity model

²⁶ E. U. Condon and G. H. Shortley, *The Theory of Atomic Spectra* (Cambridge University Press, Cambridge, England, 1935), pp. 189-191.

²⁷ J. Bardeen, L. N. Cooper, and J. R. Schrieffer, *Phys. Rev.* **108**, 1175 (1957).

²⁸ P. A. Seeger, in *Proceedings of the Third International Conference on Atomic Masses* (University of Manitoba Press, Winnipeg, Canada, 1967), p. 85.

²⁹ S. Wahlborn, *Nucl. Phys.* **37**, 554 (1962).

²⁵ J. R. Grover, *Phys. Rev.* **123**, 267 (1961); **127**, 2142 (1962).

TABLE I. Shell models used in calculations.

Protons		Seeger		Neutrons		Nilsson		ΔE_N ($\text{MeV} \times A^{1/3}$) Nilsson- Seeger
Number in shell	Energy ($\text{MeV} \times A^{1/3}$)	Number in shell	Energy ($\text{MeV} \times A^{1/3}$)	Number in shell	Energy ($\text{MeV} \times A^{1/3}$)	Number in shell	Energy ($\text{MeV} \times A^{1/3}$)	
2	0.0	2	0.0	2	0.0	2	0.0	0.0
4	28.8	4	30.9	4	30.9	4	39.0	8.1
2	41.1	2	46.7	2	46.7	2	45.1	-1.6
6	57.3	6	62.7	6	62.7	6	77.9	15.2
4	73.6	2	78.8	2	78.8	2	82.0	3.2
2	75.9	4	83.6	4	83.6	4	88.2	4.6
8	85.4	8	94.7	8	94.7	8	108.3	13.6
6	104.6	4	112.6	4	112.6	4	119.5	6.9
4	107.9	6	119.4	6	119.4	6	122.6	3.2
10	113.1	2	123.2	2	123.2	2	125.7	2.5
2	116.2	10	126.7	10	126.7	10	137.4	10.7
8	134.7	6	146.2	6	146.2	6	154.4	8.2
6	138.7	8	154.5	8	154.5	8	155.8	1.3
12	140.5	2	158.0	2	158.0	2	164.0	6.0
4	150.8	12	158.6	4	158.6	4	164.6	6.0
2	152.5	4	161.6	12	161.6	12	167.1	5.5
10	164.1	8	179.4	8	179.4	8	187.8	9.4
14	167.6	10	189.0	10	189.0	10	189.6	0.6
8	168.8	14	190.5	14	190.5	14	195.0	4.5
6	183.8	4	193.4	4	193.4	4	201.1	7.7
4	186.4	6	198.7	6	198.7	6	202.1	3.4
2	192.8	2	201.7	2	201.7	2	207.3	5.6
12	193.0	10	212.4	10	212.4	10	219.4	7.0
16	194.5	16	222.3	16	222.3	16	221.6	-0.7
10	198.1	12	223.0	12	223.0	16	226.7	3.7
8	215.7	6	228.3	6	228.3	6	236.4	8.1
6	219.0	8	235.0	8	235.0	8	237.8	2.8
18	221.1	2	237.9	2	237.9	2	246.0	8.1
14	221.4	4	240.8	4	240.8	4	246.6	5.8
12	226.9	12	245.3	12	245.3			
4	228.7	18	253.9	18	253.9			

does not apply. This is not completely correct since at equally high energies, for configurations with little or no blocking, Eqs. (5) to (7) can be solved. The breakdown of the model should be described as configuration dependent rather than energy dependent; however, the high-energy cases with real solutions are rare compared to the ones without real solutions.³⁰ In our computations, when real solutions could not be obtained, $\Delta=0$ was assigned.

The BCS prescription does not tell us what to do about configurations involving promoted pairs. Each BCS solution as obtained implies a unique probability distribution of paired nucleons among the unblocked orbitals and reflects only the configuration of the unpaired nucleons. The excitation energy for configurations that include promoted pairs was estimated by adding to the BCS energy the difference in single-particle energies of the particular configuration of pairs and that configuration of pairs where the pairs were all placed in the lowest available unblocked orbitals. It is anticipated that the error inherent in the above estimate is not very serious since we have

³⁰ H. J. Mang, J. K. Poggenburg, and J. O. Rasmussen, Nucl. Phys. 64, 353 (1965). These authors found that the occurrence of trivial solutions is due to approximations used to obtain the BCS equations, and that, without these approximations (but with others), real positive Δ 's can be obtained.

found that (for ⁷⁶Br, for example) the fractional number of levels with pair excitations increases to ~ 0.4 at very high level densities, so that, on the average, the fraction of excitation energy contributed by pair excitations is small [e.g., see Figs. 15(a) and 15(b), given later].

Since it is necessary to find the BCS solution only for different configurations of unpaired nucleons, and only unpaired nucleon configurations are required for the determination of the corresponding spin distributions, it proves convenient to use two interacting odometers, one for excited-pair configurations and one for unpaired-particle configurations.

B. Input Values

The single-particle model of Nilsson³¹ was used, the ordering of single-particle levels and energies being obtained from Seeger.³² Calculations were also made using Nilsson's energies to see the effects arising from differences in the ordering of the single-particle levels and in the relative energies. The single-particle level ordering and the corresponding energies and energy comparison are given in Table I. The most significant

³¹ S. G. Nilsson, Kgl. Danske Videnskab. Selskab, Mat.-Fys. Medd. 29, 16 (1955).

³² We are indebted to Dr. Seeger for sending us his unpublished single-particle energies.

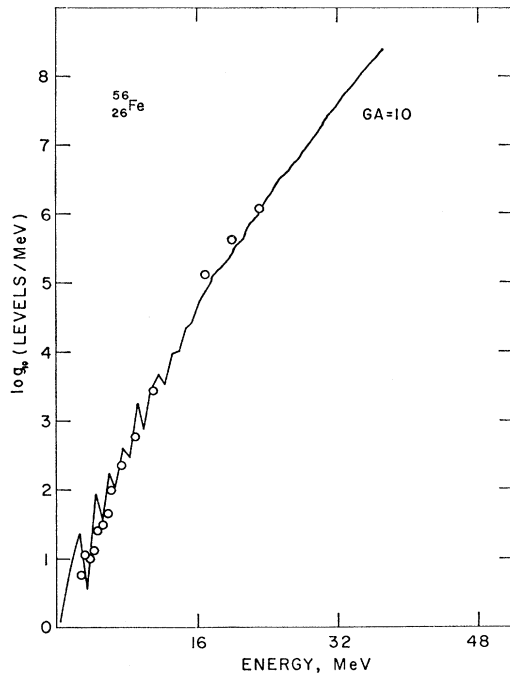


FIG. 3. Level density of ^{56}Fe ; the jagged curve is the calculated level density; the circles are the experimental points.

difference between Nilsson's and Seeger's levels is in the spacing of levels, as shown by the wide range of ΔE .

Because of space and time limitations in the computer, the calculations were arbitrarily limited to include 31 subshells, comprising 226 orbitals for the protons and 214 for the neutrons. This limitation consequently imposes a maximum energy for which all of the levels could be determined (the energy for which one nucleon is promoted to the highest included orbital). Since many more high-energy levels are contributed by complex configurations than by configurations in which one nucleon is promoted to a very high energy, no significant amount of information is lost in calculations for energies not too far above the assured maximum. Some of the calculations carried out for heavy nuclides were for energies somewhat above the assured maximum.

Other workers have treated the choice of the number of orbitals differently. For example, Seeger²⁸ used 30 orbitals straddling the Fermi level, Baranger³³ used two major oscillator shells, and Grover⁶ used one major shell. We chose to use the entire nucleus in which we considered possible configurations. This choice avoids the problems that arise in treating configurations with orbitals outside the range of the BCS calculations.

The parameter G is traditionally determined as that value which gives the correct energy gap for the mass surface. In this way we estimated G to be ap-

³³ M. Baranger and K. Kumar, Nucl. Phys. **A110**, 529 (1968).

proximately $10/A$ to $12/A$, although large deviations were noted at low A . These values are smaller than those usually used, of course, since G is dependent on the number of orbitals used in the BCS calculation and we used many more than most workers do.

Perhaps it is useful at this point to summarize briefly the most important features of the model and approximations that we used. These are

- (1) infinitely deep spherical well, with Seeger's choice of single-particle eigenvalues,
- (2) truncation of single-particle eigenvalues at 31 subshells,
- (3) zeroth-order approximation for promoted pairs,
- (4) summation range of BCS equations taken over entire assumed set of orbitals,
- (5) use of the same value of G for both neutrons and protons, and for all orbitals,
- (6) omission of p - n forces.

V. COMPARISON: NUMERICAL CALCULATIONS WITH EXPERIMENT

Level densities are known³⁴⁻³⁶ for the nuclei ^{56}Fe and ^{55}Mn for excitation energies from 0 to 23 MeV. For no other nuclei are level densities known over such a wide span of energies, at present. Comparisons of calculations with the experimental results are given in Figs. 3 and 4. A value of $GA=10$ was used for

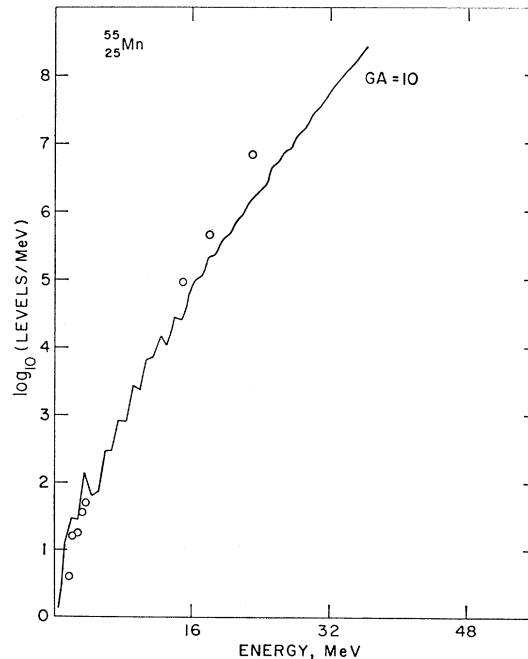


FIG. 4. Level density of ^{55}Mn ; the jagged curve is the calculated level density; the circles are the experimental points.

³⁴ A. A. Katsanos, R. W. Shaw, R. Vandenbosch, and D. Chamberlin (unpublished).

³⁵ A. A. Katsanos, Argonne National Laboratory Report No. ANL-7289, 1967 (unpublished).

³⁶ J. R. Huizenga, H. K. Vonach, A. A. Katsanos, A. J. Gorski, and C. J. Stephen (unpublished).

both in accordance with what is believed to be a reasonable value in that region of masses. The agreement with the ^{55}Mn data is satisfactory and that with the ^{56}Fe data is very good. It should be noted that the higher-energy experimental points were determined using an assumed spin distribution which we consider invalid (*vide infra*). Adjustments of the experimental data should be made accordingly, but would be too small to alter our conclusion significantly.

Level densities near neutron binding energies have been measured^{2,4,5,37} for many nuclei throughout the chart of nuclides, and these data present a challenge for any prescription for calculating level densities over a wide range of masses and a modest range of spins. However, rather than make direct comparisons for some assumed value of G , we elected to find, for each nucleus, the value of G necessary to cause the calculated level density for the appropriate spins to pass through the experimental level density. Ideally, assuming we start with a suitable set of single-particle eigenfunctions, our calculation makes possible a method for the determination of G that is independent of the method that uses the properties of the ground and lower excited states. The results for 192 nuclides are plotted with respect to proton number in Fig. 5(a) and neutron number in Fig. 5(b). Aside from wide scatter near closed shells, the values we find are gratifyingly close to those we found previously from the ground-state energy gap. We see immediately, however, that GA is not constant in over-all trend, though it does not vary strongly with Z or N . In the calculations, G was assumed independent of nucleon type; this, too, appears to be untrue. Since GA is an increasing function with increasing Z or N , we may set $G \propto A^{-F}$, where $F < 1$. We find $GA^{2/3}$ to be approximately constant (Fig. 6). Moreover, with $F = \frac{2}{3}$ the dependence of G on the type of nucleon disappears.

It is easy to see one reason why G should not be strictly inversely proportional to the nuclear volume, i.e., to A . Since the pairing force is of short range, it operates effectively over a volume small compared with that of the nucleus. This small volume should be compared with the effective volume of the orbitals involved, rather than with the volume of the nucleus as a whole. The volumes of these orbitals will not, in general, scale exactly as A^{-1} , because they contract as they sink down in the potential. Another reason for this apparent effect can be that it is a reflection of the difference between the assumed model and real nuclei, and thus to be at least to some extent, an artifact.

In those areas where the values of G are most scattered, are exceptionally low, or are exceptionally high, the single-particle level spacing is large (i.e.,

light nuclides and/or closed shells). In these cases the sensitivity of the calculated level density to G is small. Large errors are thus associated with G in those areas. It remains to be seen if other prescriptions for the single-particle levels give different or improved results. On the other hand, the lack of sensitivity is probably associated with the large spacing of single-particle eigenvalues and, in the case of very light nuclides and at the closed shells, a breakdown of the BCS treatment. Also, the neglected p, n forces are expected to be most strongly felt in light nuclei.

A comparison that stresses another feature of nuclear level density—namely, its detailed dependence on small changes in nucleon number—is given in Table II, where we give experimental and calculated values of the density of levels of spin $\frac{1}{2}$ near the neutron binding energies of ^{55}Fe , ^{57}Fe , ^{59}Ni , and ^{61}Ni . These are unusual because, although they are all odd-mass nuclei and form three pairs that differ only by two neutrons or two protons, their level densities show striking variation.³⁸ The energies at which the measurements were made differ for each pair by 1.2 to 1.6 MeV. The Bethe formula would predict that the level densities for these nuclei should look much alike, that is, at the indicated energy differences the measured level densities should increase by factors of 3 to 6 in proceeding from the lower energies to the higher. On the other hand, our calculation explains the observed pattern quite naturally. This effect is independent of the pairing parameter. It is of interest to note that these results suggest that a dependence on nucleon valency (i.e., number of nucleons or nucleon holes away from the closed shell) seems to be showing up at excitation energies of 8–10 MeV; a valency of 3 for ^{55}Fe and ^{59}Ni and 5 for ^{57}Fe and ^{61}Ni . This is reminiscent of an effect described by Rosenzweig²³ for cases involving individual subshells, specifically the $g_{9/2}$ subshell. Our effect, however, involves several subshells, as may be seen from Table I.

VI. COMPARISON: NUMERICAL WITH ANALYTICAL CALCULATIONS

In this section we compare the results of the numerical calculations with those obtained using the algebraic formula already discussed. The analytical prescription chosen was that of Gilbert and Cameron,² primarily because of the large amount of recent data used to fix its parameters. No comparison was made with other formulas.

For the comparisons, the computed results for ^{114}Cd and ^{166}Ho were chosen because (a) their level densities are known both at low energies and near the neutron binding energies, (b) they are in areas where there is not too much scatter in the $GA^{2/3}$ versus N or P curve, and (c) one is an even-even nuclide near

³⁷ Brookhaven National Laboratory Report No. 325 (U.S. Government Printing Office, Washington, D.C., 1966), 2nd ed., Suppl. No. 2.

³⁸ We are indebted to Professor J. R. Huizenga for suggesting that we use this problem to test our calculations.

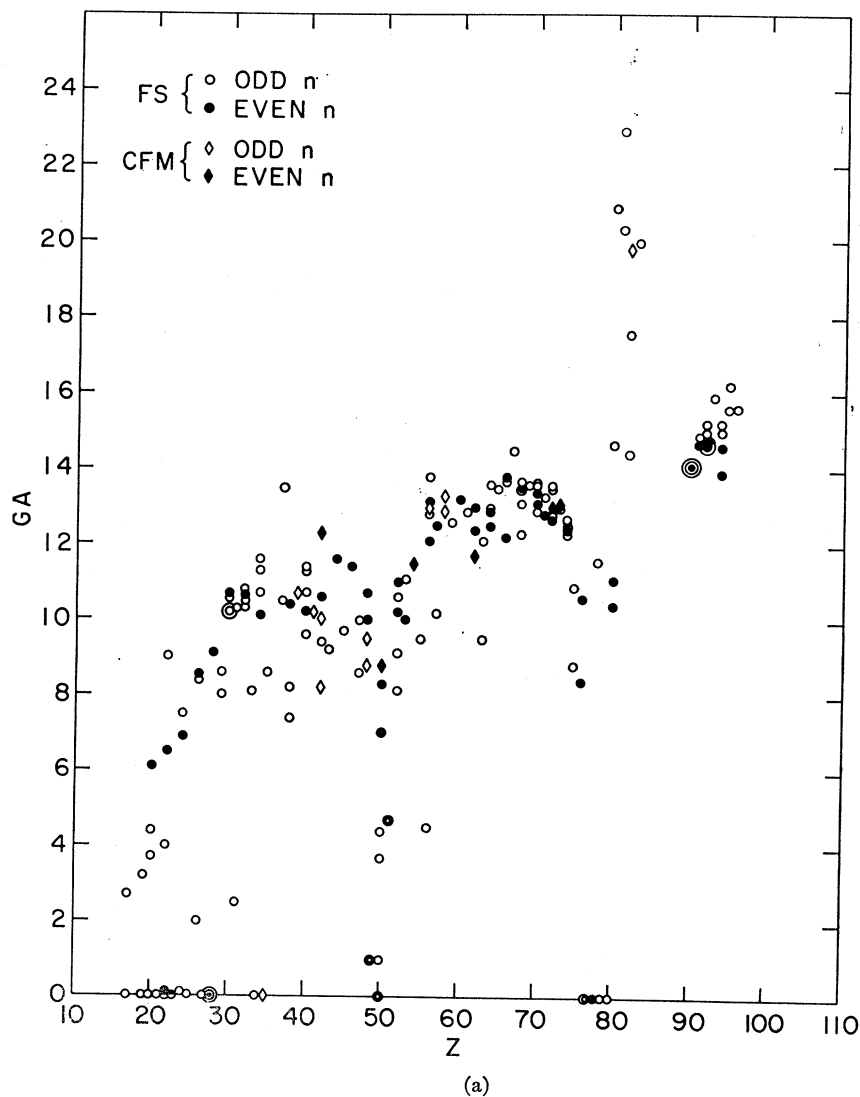


FIG. 5. Values of GA that cause the calculated level densities to fit the experimental level densities at the neutron binding energies; (a) versus proton number; (b) versus neutron number. FS, experimental data from Ref. 4; CFM, experimental data from Ref. 5.

a major closed shell, while the other is an odd-odd nuclide far from a closed shell. To look for the main effects of proximity to closed shells, these two nuclides appear to be good candidates for comparison.

The best values of G were determined for both nuclides and all results are for these values. It should be noted that $GA=14.5$ for ^{166}Ho is a little higher than for the neighboring nuclides. In Figs. 7 and 8 are given (a) the known experimental points,^{4,39} (b) the calculated level densities for two different values of G , (c) the calculated level densities using Nilsson's³¹ energies and order of levels, and (d) the calculated level densities according to the algebraic formula. The experimental neutron resonance points have been cor-

rected to total level densities according to the spin distribution given by the numerical method. If corrected for the spin distribution used by the algebraic formula, then the corrected neutron resonance point lies on that curve.

We find significant differences using Seeger's energies and Nilsson's energies, and a marked difference in shape between the numerical and algebraic curves for ^{114}Cd , while the two curves for ^{166}Ho are very similar.

In the low-energy part of the curve for ^{166}Ho , blown up on the right-hand side of Fig. 8 as an integral, a large difference appears in the number of levels near the ground state, depending on whether Seeger's or Nilsson's single-particle levels are used. This is caused by the ordering of the single-particle levels and is corollary to the Rosenzweig effect.²³

Greater insight to the comparison with the alge-

³⁹ *Nuclear Data Sheets*, compiled by K. Way *et al.* (National Academy of Sciences—National Research Council, Washington, D.C., 1965).

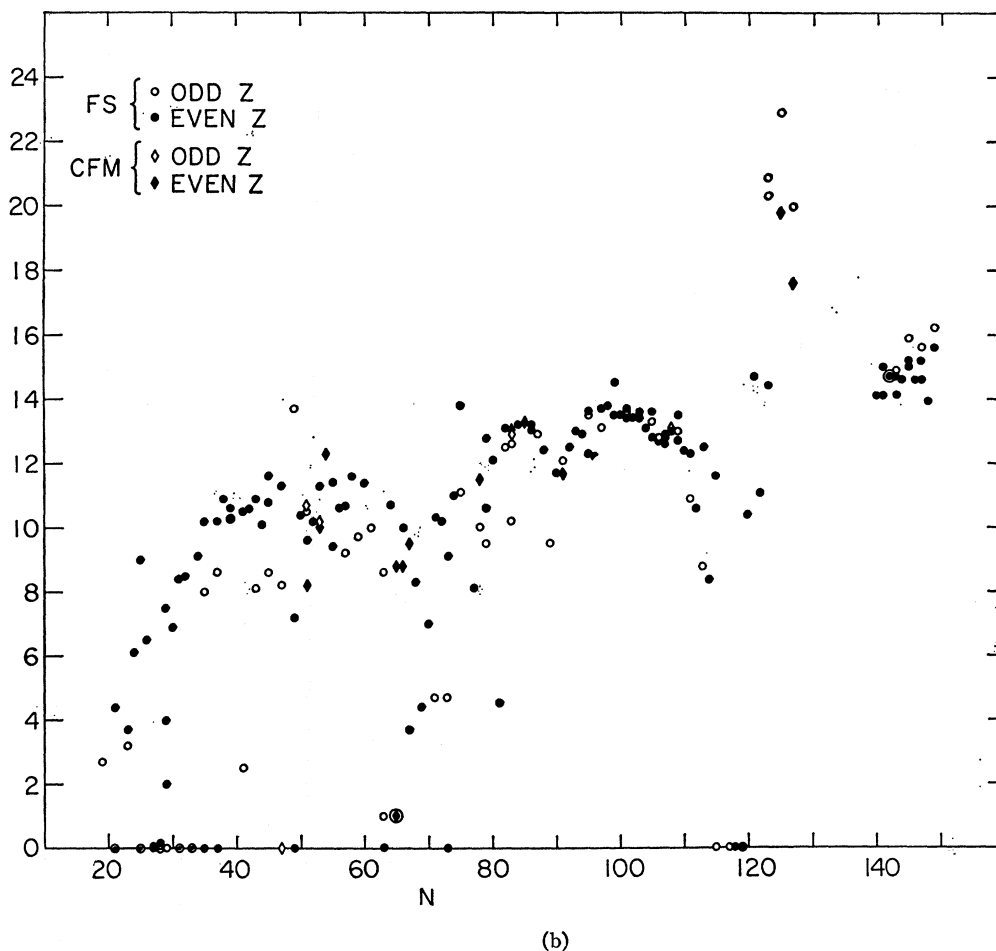


FIG. 5. (Continued).

braic formula can be obtained in Figs. 9(a) and 9(b) and 10(a) and 10(b). In the first pair of figures the \log_{10} of the level densities versus energy and spin are plotted as contours. The yrast levels, which fall naturally out of the calculations, are given by dashed

lines in the figures. In the second pair of figures, contours of the \log_{10} of the ratios of the numerically (ω_H) and algebraically (ω_C) calculated spin-dependent level densities are plotted. For ^{166}Ho , all of the contours are essentially energy independent, indicating, as in Fig. 8, that the agreement is good for the energy dependence. However, very large discrepancies appear in the spin dependence. For ^{114}Cd , marked discrepan-

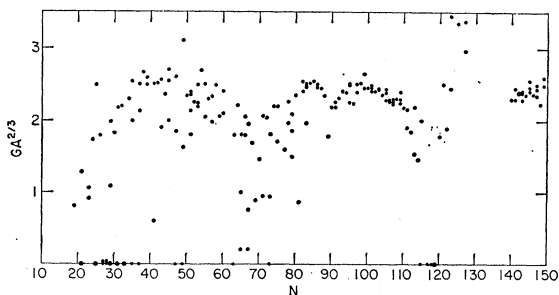
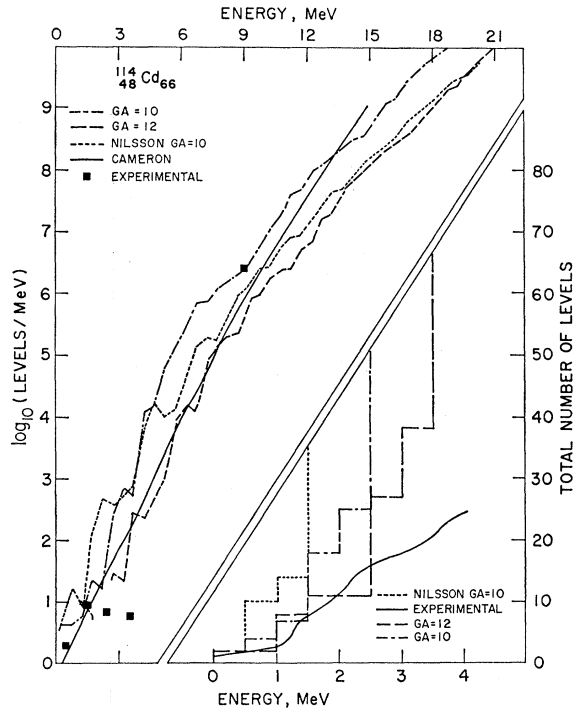


FIG. 6. Values of $GA^{2/3}$ that cause the calculated level densities to fit the experimental level densities at the neutron binding energies; versus neutron number.

TABLE II. Effect on level densities of adding pairs of nucleons.

Nucleus	Average energy (MeV)	Experimental level density (levels per MeV)	Calculated level density		
			GA^2	6	10
$^{56}\text{Fe}_{28}$	9.55	40 ± 9	57	41	28
$^{57}\text{Fe}_{24}$	7.96	39 ± 8	89	60	41
$^{59}\text{Ni}_{23}$	9.30	44 ± 9	28	38	26
$^{61}\text{Ni}_{23}$	8.12	51 ± 9	56	43	22

FIG. 7. Level densities of ^{114}Cd .

cies occur for both energy and spin dependence. No simple adjustment of the parameters a and δ in the algebraic formula can reproduce these. The energy-dependent differences, therefore, apparently reflect the proximity of the closed shell. Gilbert and Cameron² reported difficulties in the analytic method near closed shells.

Another effect attributable to the closed shell is a wave superimposed on the level-density curve of ^{114}Cd . This wave also appears in Figs. 11–14 (to be discussed below) and in the total level-density curves of indium and antimony nuclides, displaced by one-quarter of a wave length, and in tellurium nuclides, displaced by one-half of a wave length. These waves arise from the closed 50-proton shell as follows. In ^{114}Cd a number of configurations can be obtained without promotion of a proton above the 50-proton shell. As soon as this promotion takes place, however, a large number of additional configurations becomes available immediately and with a very small increase in energy, causing at this point a relatively steeply rising level-density curve. The curve then returns to a “normal” slope until the next proton is promoted. The displacement of waves in the other nuclides is consistent with the stage at which a proton must be promoted above the closed shell, the wavelength being consistent with the energy jump at the closed shell, about 4 MeV. This phenomenon may be an artifact of the model; it is an interesting area for future experiments.

Since both ^{166}Ho and ^{114}Cd ratios (Figs. 9 and 10) depend strongly on spin, the spin-dependent part of the level-density formula evidently contains inadmissible approximations. One of these approximations is the modified-gaussian form of the spin dependence as described in Sec. III. Another is the assumed relation of the parameter σ to the “rigid-body moment of inertia,” which also involves the simplifications described in Sec. III.

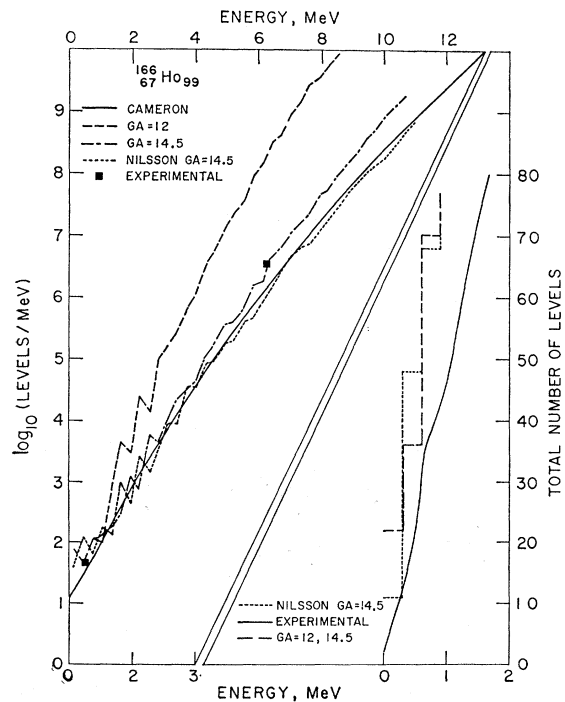
It is instructive to see what behavior is required of an assumed constant “moment of inertia” \mathcal{I} [where $\sigma^2 = \mathcal{I}\hbar^{-2}(E/a)^{1/2}$] to cause Eq. (10) to agree with the numerical solution. We therefore differentiate Eq. (10) with respect to E and J to obtain

$$\partial \ln \omega / \partial E = -2E^{-1} + a^{1/2} E^{-1/2} + [\hbar^2 J(J+1) / 4\mathcal{I}] a^{1/2} E^{-3/2}, \quad (13)$$

$$\partial \ln \omega / \partial J = 2(2J+1)^{-1} - [\hbar^2 a^{1/2} E^{-1/2} (2J+1) / 2\mathcal{I}]. \quad (14)$$

These equations can be solved for \mathcal{I} and a in terms of the slopes with respect to E and J at all points on the calculated level-density surface. Contour maps for a and $\mathcal{I}/\mathcal{I}_{\text{rigid}}$ ($r_0 = 1.2 \times A^{1/3}$ fm) for ^{114}Cd are given in Figs. 11 and 12 and for ^{166}Ho in Figs. 13 and 14.

For both isotopes the parameters \mathcal{I} and a show definite spin dependence, suggesting more clearly that the modified-gaussian representation of the spin dependence is not a particularly reliable approximation (see Appendix B). Alternative forms have been sug-

FIG. 8. Level densities of ^{166}Ho .

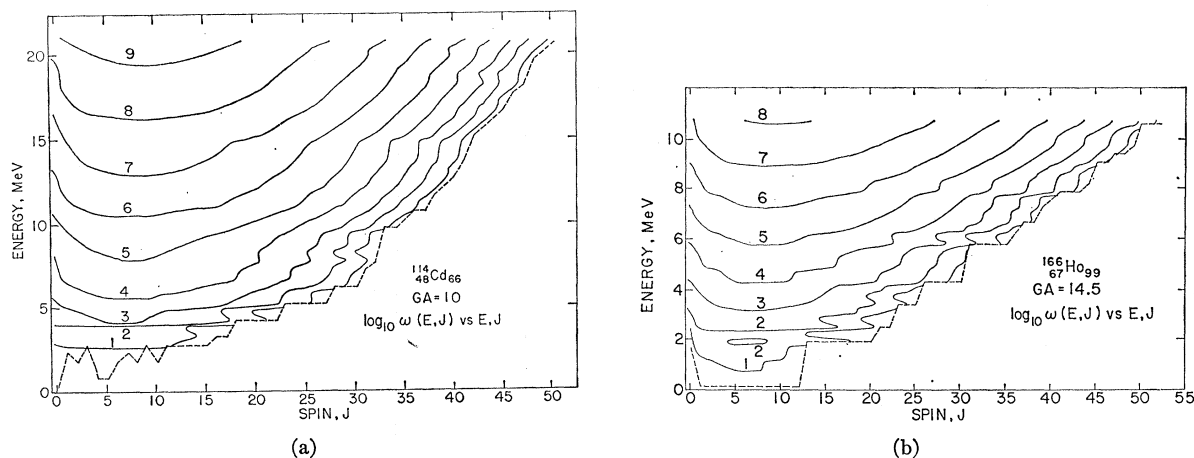


FIG. 9. Contours of level densities versus E and J . The dashed curve traces the yrast levels; (a) ^{114}Cd , (b) ^{166}Ho .

gested,⁴⁰⁻⁴³ some of which include higher-order terms in J .

In the algebraic equation discussed above the parameter a is usually assumed to be independent of energy, although some authors use an energy-dependent a . The results of the numerical calculations favor the energy-independent form, dependence on energy showing up mainly in the waves already discussed. For ^{114}Cd , a is very high at low energies, corresponding to the steep part of the first wave. This effect does not appear at all for ^{166}Ho , and the waves are much shallower.

The parameter σ is considered to be energy dependent with $\sigma^2 \propto E^{1/2}$. Contours of σ versus E and J exhibit an energy dependence that essentially dis-

appears if one assumes this proportionality through the parameter \mathcal{J} . The peculiar wiggles in the contour maps (Figs. 12 and 14) are probably associated with the energy-dependent waves and may be due to an inadequate representation of σ with respect to a .

To test the usefulness of the subtraction constant δ on excitation energy in formulas such as Eq. (10) to account for the difference between even and odd nucleon numbers, we calculated level densities up to 10^{10} levels per MeV for the quartet remote from closed shells, ^{76}Se , ^{77}Se , ^{76}Br , and ^{77}Br , using Seeger's eigenvalues and $GA=10.9$ (chosen to fit the measured slow-neutron level densities for ^{76}Se). Where $\sum_r \tau \omega(E, J) = 10^4$ to 10^5 levels per MeV (in the neighborhood of 7 MeV), the effective displacement between

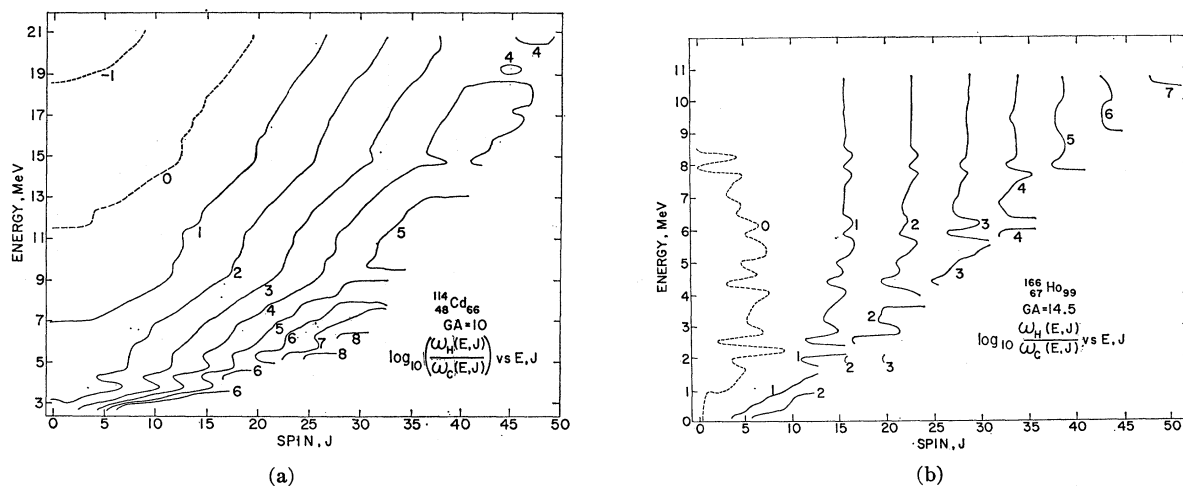


Fig. 10. Ratio of level densities calculated numerically to those calculated by algebraic formula; (a) ^{114}Cd , (b) ^{166}Ho .

⁴⁰ D. W. Lang, in *Proceedings of the Third Conference on Reactions between Complex Nuclei* (University of California Press, Berkeley, 1963), p. 248.

⁴¹ D. W. Lang, *Nucl. Phys.* **77**, 545 (1966).

⁴² T. D. Thomas, *Ann. Rev. Nucl. Sci.* **18**, 343 (1968).

⁴³ J. Gilat (private communication and unpublished work).

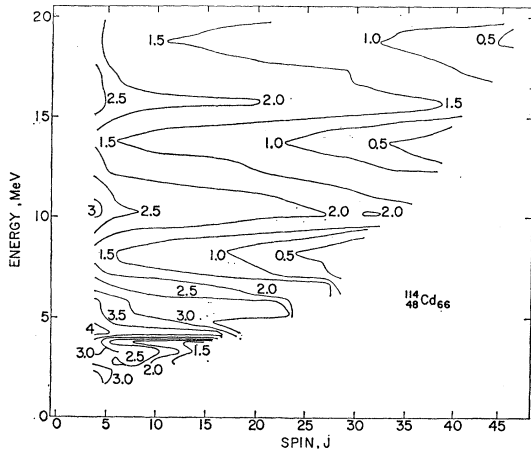


FIG. 11. Contours of g/g_{rigid} versus E, J for ^{114}Cd .

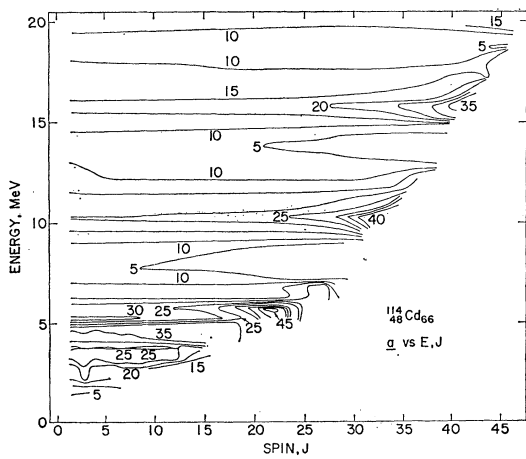


FIG. 12. Contours of a versus E, J for ^{114}Cd .

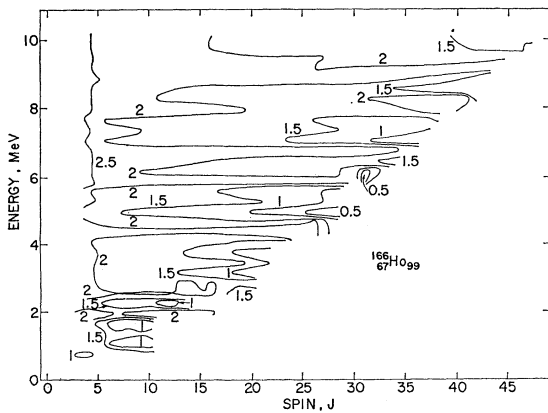


FIG. 13. Contours of g/g_{rigid} versus E, J for ^{166}Ho .

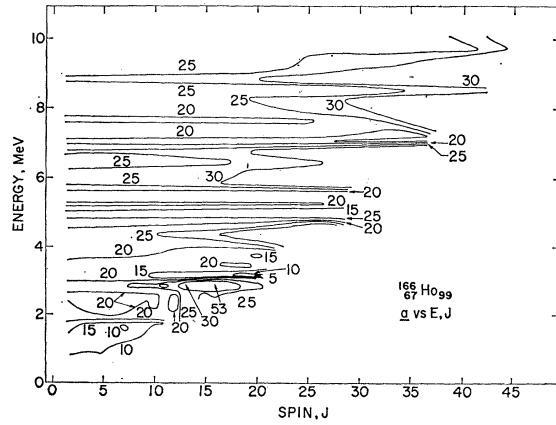


FIG. 14. Contours of a versus E, J for ^{166}Ho .

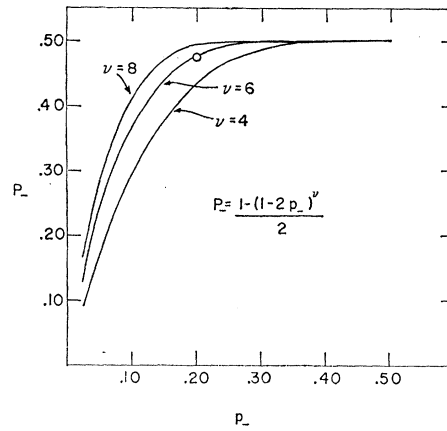


FIG. 15. The probability of a negative-parity state (P_-) determined from the abundance of negative-parity single-particle levels (p_-), and the number of unpaired particles (ν).

TABLE III. Ratios of + parity to - parity.

E (MeV)	^{114}Cd	E (MeV)	^{166}Ho
0.5	1.00	0.45	0.94
1.5	2.50	1.35	1.43
2.5	0.47	2.25	1.14
3.5	1.47	3.15	1.02
4.5	1.07	4.05	1.05
5.5	1.08	4.95	1.00
6.5	1.00	5.85	1.07
7.5	0.89	6.75	1.04
8.5	1.17	7.65	1.01
9.5	0.88	8.55	1.05
10.5	0.95	9.45	0.96
11.5	1.16	10.35	1.06
12.5	0.87		
13.5	1.04		
14.5	0.94		
15.5	1.05		
16.5	1.02		
17.5	0.92		
18.5	1.04		
19.5	1.00		
20.5	0.94		
Total	0.97		1.03

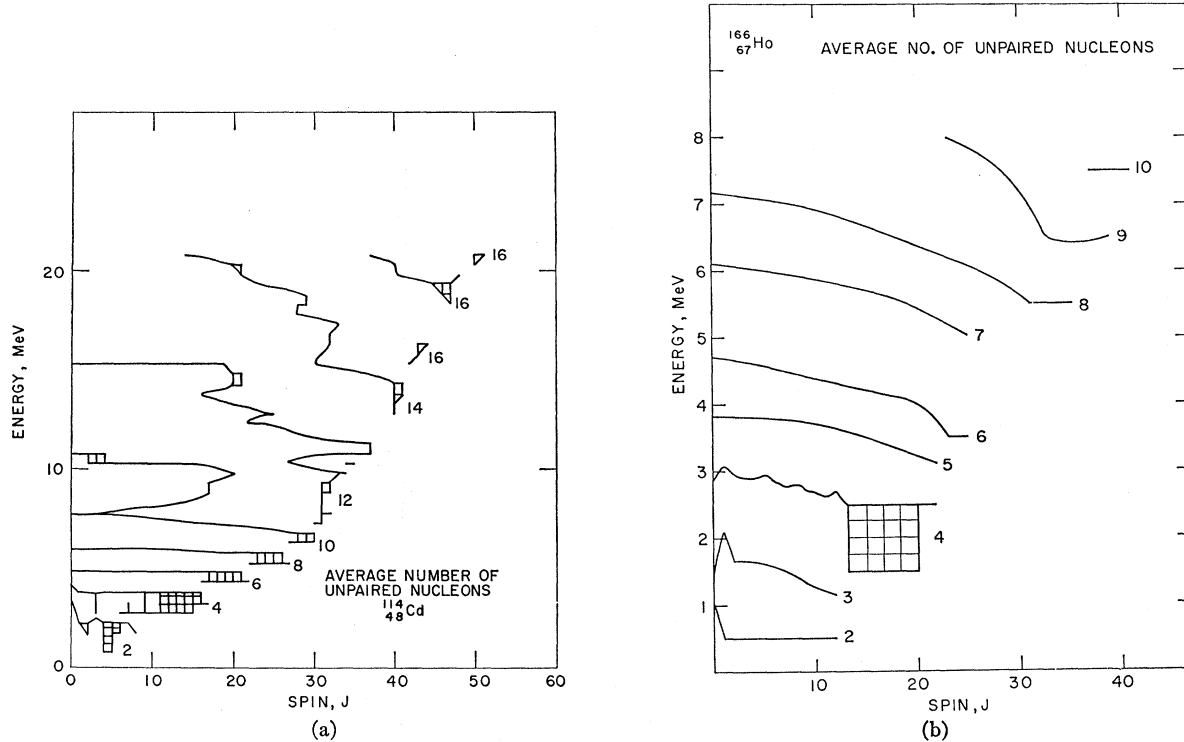


Fig. 16. Average number of unpaired particles versus E and J ; (a) ^{114}Cd , (b) ^{166}Ho .

even-even ^{76}Se and odd-odd ^{76}Br is 2.3 MeV. The two curves diverge gradually until at 10^9 to 10^{10} levels per MeV (in the neighborhood of 25 MeV) the displacement is 3.5 MeV. Thus, for narrow energy regions the assumption of a constant displacement is probably useful, but over a wide energy region an important correction would be needed.

However, although the odd-mass level densities fall between the above two curves, they do not coincide for their entire length; they coincide below about 10^9 levels per MeV, but the curve for ^{77}Br is displaced above the curve for ^{77}Se by energies varying from 0.5 to 1.7 MeV. Thus, we see that effects due to specific subshell positioning are as large as the divergence mentioned in the previous paragraph, precluding any all-embracing prescription. It should also be recalled that it is in the region far from closed shells that level densities are the most sensitive to the value of G ; tolerance of only a small variability of G from nucleus to neighboring nucleus would render it even more difficult to make a general statement about the energy dependence of the pairing correction δ .

One other result of the numerically computed level densities that can be compared to previous approximations is the distribution of parities. Ericson³ has demonstrated that the number of levels of both parities should be nearly equal. We find that this is roughly correct, but there are notable deviations (Table III). These deviations are even greater (up to 30%) when the spin-dependent level densities are compared. In

Fig. 15 are given Ericson's expected parity probabilities for various numbers of unpaired particles. It is clear from this figure that our results are not unexpected. The single point used by Ericson for his demonstration is shown by the circle.

It is also interesting to examine the average number of unpaired particles that contribute to the level densities at each E and J . This parameter arises in various analyses of the spin distributions as well as in the discussion of parity distribution above. Contours versus energy and spin are shown in Figs. 16(a) and 16(b) for ^{114}Cd and ^{166}Ho , respectively. The average number of unpaired particles increases at constant energy with increasing spin.

VII. CONCLUSION

We have attempted by exact calculations to find what the model usually used for level densities predicts. We have compared these results with those obtained from the traditional algebraic formulation to reveal the shortcomings of the latter. The most significant shortcomings are (a) incorrect logarithmic curvature of the energy dependence of the total level density, (b) omission of nonuniform features and an energy-dependent wave, arising from the nuclear shell structure, superimposed on the over-all level density, and (c) incorrect spin distributions. The last is the most serious of all, especially for use in analysis of high-energy reactions. Alternative algebraic forms are

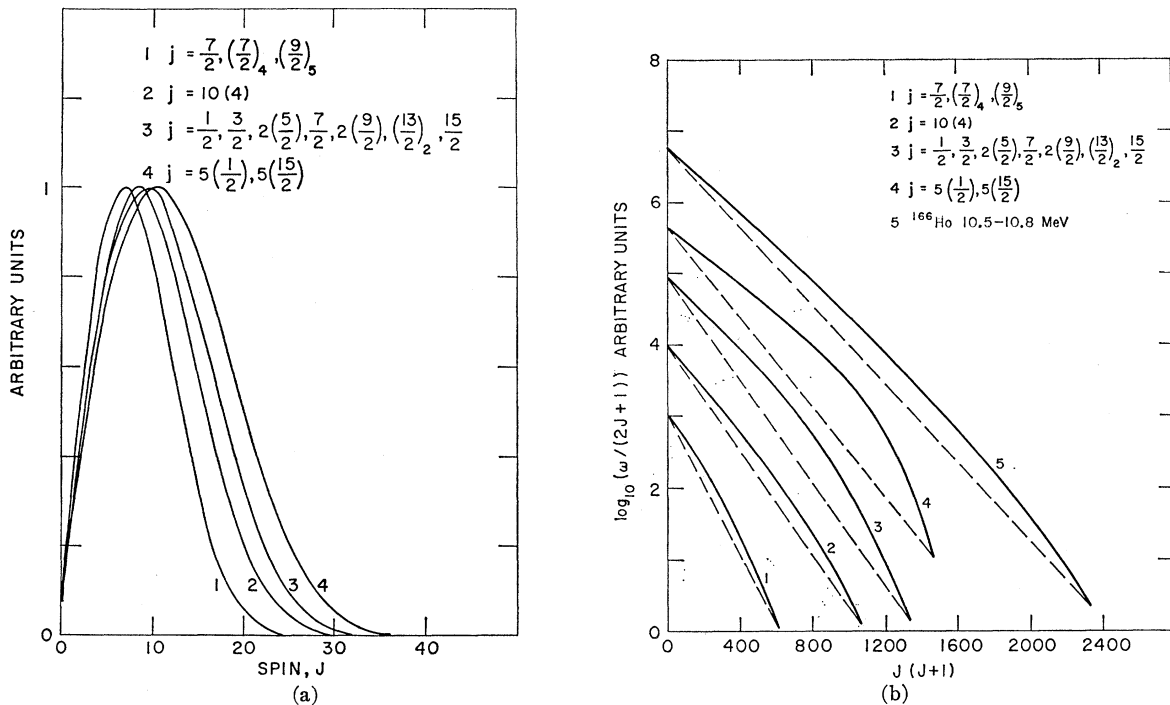


FIG. 17. (a) The spin distributions obtained from various admixtures of spins of single-particle states; (b) demonstration of unsuitability of the modified-Gaussian representation.

being sought and will be described in subsequent papers.

Note added in proof. While this paper was at the compositor, an error was found in the computer program. All of the calculations reported here were repeated, but the differences found were too insignificant to warrant replacement of the figures, and no conclusions were changed.

ACKNOWLEDGMENTS

We are pleased to thank Professor Guy Emery for his interest and helpful discussions, Professor Robert Vandenbosch for his helpful comments and criticism, and Duane Davis for assistance with some of the computations.

APPENDIX A: MAYER-JENSEN TABLE OF TOTAL SPIN

For identical nucleons in a subshell, only those states are permitted for which the Pauli exclusion principle is obeyed, so that we cannot use the simple vectorial method described in Sec. IV A 1 for calculating the distribution of levels with respect to spin. For rapid calculations a useful method for handling this problem is to look up the required spin distributions in a table, such as the one given by Mayer and Jensen.⁴⁴

However, their table only gives distributions for spins of subshells through $j = \frac{1}{2}$, which is not adequate

⁴⁴M. G. Mayer and J. H. D. Jensen, *Elementary Theory of Nuclear Shell Structure* (John Wiley & Sons, Inc., New York, 1955).

for our purpose since we used subshells with spins up to $j = \frac{1}{2}7$. The spin distributions for all configurations for $j \leq \frac{9}{2}$ were, therefore, computed by the modification appropriate for j - j coupling of the method outlined in the text by Condon and Shortley.²⁶ The entire table is reproduced here (Table IV). It should be noted that only three errors were found in the Mayer-Jensen hand-calculated table.

As in the Mayer-Jensen table, the table here gives the number of times each spin J occurs for various configurations $(j)^k$, where \mathbf{j} is the spin of the subshell and k is the number of identical nucleons in the subshell. The numbers are given only for those spins that are appropriate according to the evenness or oddness of k . Thus, for k odd, the columns from left to right are for spins $\frac{1}{2}, \frac{3}{2}, \frac{5}{2}$, etc., but for k even, the same columns should be understood to be for spins $0, 1, 2, 3, \dots$.

In the level-density calculations we required the spin distribution for $(j)^{k'}$, where k' is the number of unpaired nucleons. This result is clearly given by the difference of the spin distributions of $(j)^k$ and $(j)^{k-2}$, because simply adding a nucleon pair to configurations $(j)^{k-2}$ contributes no additional spins, and therefore the configurations $(j)^{k-2}$ account for spins for the configurations $(j)^k$ which contain at least one pair.

APPENDIX B: MODIFIED-GAUSSIAN SPIN DEPENDENCE

Thomas⁴² has indicated that discrepancies exist between the simple assumed modified-Gaussian spin

TABLE IV. Mayer-Jensen table.

J	K	Number of times each spin occurs										
		1	0	1	0	1	0	1	0	1	0	
3/2	2	1	0	1								
	5/2	2	1	0	1	0	1					
7/2	3	0	1	1	0	1						
	4	1	0	2	0	2	1	0	1	1	0	
	9/2	2	1	0	1	0	1	0	1	0	1	
9/2	3	0	1	1	1	2	1	1	1	1	0	
	4	1	0	2	1	3	1	3	1	2	1	
	5	1	1	2	2	3	2	2	2	2	1	
	6	1	0	1	0	1	0	1	0	1	0	
	11/2	3	0	1	1	1	2	2	1	2	1	1
11/2	4	1	0	3	1	4	2	4	2	4	2	
	5	1	2	3	4	4	5	4	5	4	4	
	6	3	3	2	2	1	1	0	1	1	0	
	7	3	0	4	3	6	3	7	4	6	4	
	8	5	2	4	2	2	1	1	0	1		
	13/2	2	1	0	1	0	1	0	1	0	1	0
	13/2	3	0	1	1	1	2	2	2	2	2	1
4		2	1	1	1	1	0	1	1	3	6	
5		2	0	4	1	5	3	5	3	6	3	
6		5	3	4	2	3	1	2	1	1	0	
7		1	3	5	5	7	7	8	8	8	7	
8		8	6	6	5	5	3	3	2	2	1	
9		1	0	1								
10		4	1	7	5	11	7	13	9	13	10	
13/2	11	12	8	11	7	8	5	6	3	4	2	
	12	2	1	1	0	1						
	13	3	4	7	9	10	11	13	12	13	12	
	14	12	10	11	8	8	6	5	4	4	2	
15/2	2	1	0	1	0	1	0	1	0	1	0	
	3	0	1	1	1	2	2	2	3	2	2	
	4	2	2	1	2	1	1	1	1	0	1	
	5	3	0	4	2	6	3	7	4	7	5	
	6	7	4	7	4	5	3	4	2	3	1	
	7	2	1	1	0	1						
	8	2	4	6	8	9	11	11	13	12	13	
	9	12	12	11	11	9	9	7	7	5	5	
	10	3	3	2	2	1	1	0	1			
	11	6	2	11	9	17	13	22	17	23	19	
15/2	12	24	18	23	17	19	15	16	11	13	8	
	13	9	6	6	3	4	2	2	1	1	0	
	14	1										
	15	4	10	13	17	21	24	25	29	28	29	
	16	29	29	26	27	23	22	19	18	14	14	
	17	10	9	7	6	4	4	2	2	1	1	
15/2	18	0	1									
	19	7	4	16	13	25	21	31	26	35	29	
	20	35	29	34	27	30	23	25	19	20	14	
	21	15	10	10	6	7	4	4	2	2	1	
	22	1	0	1								
17/2	2	1	0	1	0	1	0	1	0	1	0	
	3	0	1	1	1	2	2	2	3	3	2	
	4	3	2	2	2	2	1	2	1	1	1	
	5	1	0	1								
17/2	6	3	0	5	2	7	4	8	5	9	6	
	7	9	6	9	6	8	5	7	4	5	3	

TABLE IV (Continued)

<i>J</i>	<i>K</i>	Number of times each spin occurs									
17/2	5	4	2	3	1	2	1	1	0	1	
		3	5	8	10	13	14	16	17	19	18
		19	18	19	17	17	15	15	13	12	10
	6	10	7	7	5	5	3	3	2	2	1
		1	0	1							
		8	4	16	14	26	21	34	28	37	33
	7	40	33	41	33	37	31	34	26	29	22
		23	18	18	12	14	9	9	6	6	3
		4	2	2	1	1	0	1			
	8	8	16	24	31	38	43	49	52	57	57
		60	59	60	57	57	52	51	46	44	38
		36	30	28	23	21	16	15	11	10	7
	9	6	4	4	2	2	1	1	0	1	
		12	10	32	30	51	48	66	61	77	70
		83	74	84	74	80	69	74	62	64	53
	10	54	43	43	33	33	25	24	17	17	11
		11	7	7	4	4	2	2	1	1	0
		1									
	11	11	24	34	43	56	62	69	76	82	82
88		86	87	85	83	77	77	69	65	59	
55		46	44	36	33	27	24	18	17	12	
12	10	8	7	4	4	2	2	1	1	0	
	1										
19/2	2	1	0	1	0	1	0	1	0	1	0
		1	0	1	0	1	0	1	0	1	0
	3	0	1	1	1	2	2	2	3	3	3
		3	3	2	3	2	2	2	2	1	2
	4	1	1	1	1	0	1				
		3	0	6	2	8	5	9	6	11	7
		11	8	11	8	11	7	10	7	8	5
	5	7	4	5	3	4	2	3	1	2	1
		1	0	1							
		3	7	10	13	16	19	20	24	24	26
	6	26	27	26	27	25	25	23	23	20	20
		17	16	14	13	10	10	7	7	5	5
		3	3	2	2	1	1	0	1		
	7	10	6	23	21	37	32	49	43	56	51
		62	54	65	56	63	55	60	50	55	45
		47	39	40	31	33	25	25	19	19	13
	8	14	9	9	6	6	3	4	2	2	1
		1	0	1							
		14	26	39	53	62	74	83	91	97	105
9	106	111	111	112	109	110	103	102	95	91	
	83	80	70	66	58	53	45	42	34	31	
	25	22	17	16	11	10	7	6	4	4	
10	2	2	1	1	0	1					
	20	22	58	61	96	95	128	124	152	147	
	169	159	179	166	178	164	173	155	161	142	
11	144	126	125	106	106	88	85	70	67	53	
	51	39	37	28	26	18	18	12	11	7	
	7	4	4	2	2	1	1	0	1		
12	25	53	76	100	123	144	160	180	191	204	
	212	220	220	226	221	220	213	209	196	191	
	176	167	153	143	127	119	103	94	81	73	
13	60	55	44	39	31	27	20	18	13	11	
	8	7	4	4	2	2	1	1	0	1	
	24	32	81	85	131	136	175	175	212	205	
14	236	227	248	235	252	233	244	224	228	205	
	208	182	181	158	153	131	127	105	100	82	
	77	61	58	44	41	31	28	20	19	12	
15	12	8	7	4	4	2	2	1	1	0	
	1										
21/2	2	1	0	1	0	1	0	1	0	1	0
		1	0	1	0	1	0	1	0	1	0
	3	1									
		0	1	1	1	2	2	2	3	3	3
		4	3	3	3	3	2	3	2	2	2
	4	2	1	2	1	1	1	1	0	1	
		4	0	6	3	9	5	11	7	12	9
		13	9	14	10	13	10	13	9	12	8

TABLE IV (Continued)

J	K	Number of times each spin occurs									
21/2		10	7	8	5	7	4	5	3	4	2
		3	1	2	1	1	0	1			
	5	4	8	13	16	20	23	27	29	32	33
		36	35	37	36	37	35	35	33	33	30
		29	26	26	22	21	18	17	14	13	10
		10	7	7	5	5	3	3	2	2	1
		1	0	1							
	6	13	9	31	30	51	46	68	62	80	75
		96	81	97	87	97	88	96	84	92	79
		83	72	74	62	65	53	53	44	44	34
		35	26	26	20	19	13	14	9	9	6
	6	3	4	2	2	1	1	0	1		
7	20	42	62	80	101	116	132	147	160	168	
	181	184	191	193	196	192	194	187	184	176	
	171	159	155	141	134	122	114	101	95	82	
	75	65	59	49	45	36	32	26	23	17	
	16	11	10	7	6	4	4	2	2	1	
	1	0	1								
8	31	42	101	111	168	175	227	230	277	275	
	314	307	340	327	352	334	352	330	341	315	
	321	293	293	264	262	232	227	198	192	165	
	158	133	127	105	98	80	75	59	55	42	
	39	29	27	19	18	12	11	7	7	4	
	4	2	2	1	1	0	1				
9	51	106	157	203	254	295	337	374	408	433	
	464	478	495	505	514	510	514	502	496	480	
	467	443	430	401	381	354	333	302	283	253	
	233	207	188	163	149	126	112	95	84	68	
	61	48	42	33	28	21	19	13	11	8	
	7	4	4	2	2	1	1	0	1		
10	52	83	179	212	304	328	416	432	507	518	
	581	578	633	620	657	639	664	633	650	611	
	616	575	570	523	516	467	452	406	389	342	
	327	283	266	229	212	178	166	136	124	101	
	92	72	66	50	45	34	30	21	20	13	
	12	8	7	4	4	2	2	1	1	0	
	1										
11	72	142	212	277	343	401	459	507	555	592	
	630	653	679	690	704	703	706	693	686	664	
	649	619	598	562	537	499	470	431	402	363	
	336	299	273	240	217	187	168	142	126	105	
	93	75	66	52	45	35	30	22	19	14	
	12	8	7	4	4	2	2	1	1	0	
	1										

dependence, a sample numerical expansion of the spin distribution, and the more complete expansions carried out by Grover⁶ in his calculations of the yrast levels. These, as well as the shortcomings described in the main text arise because (1) the number of unpaired particles is too small to permit use of the central-limit theorem and (2) the vector contributions by unpaired nucleons in the same subshell are correlated, not random. We extended Thomas's development to a more realistic sample by assignment of a different spin to each nucleon instead of using a constant spin of 4, by allowing for the possibility of more than one unpaired nucleon to be in the same subshell, and also by inclusion as an example the numerical results for ¹⁶⁶Ho.

Four different configurations were taken with the same number of unpaired nucleons and with the same net average spin. If the spin distributions of the levels derived from these configurations were all of the same

nucleus, they would all represent the same temperature of that nucleus. It is clear from Fig. 17(a) that they do not represent the same "moment of inertia" of the nucleus as required by the usually-used relation between σ and ϑ . Furthermore, as far as experimental work is concerned, many different configurations with different average spins (and temperatures) fall at the same energy. If it is desirable to discuss ϑ at all, then one should probably discuss an average for a collection of nuclei.

Furthermore, Eq. (10) transforms simply to

$$\ln[\omega/(2J+1)] = A - BJ(J+1), \quad (15)$$

and, thus, at a given energy, a plot of $\ln[\omega/(2J+1)]$ versus $J(J+1)$ should give a straight line. The curvatures obtained for the energies described in Fig. 17(a) and for the calculations of ¹⁶⁶Ho at 10.5–10.8 MeV [Fig. 17(b)] show more clearly the extent of the deviations from the modified-Gaussian distribution.